ACADEMY REPORTS ONLINE!
Sign up for PNAS Online eTocs
Get notified by email when new content goes on-line

Info for Authors | Editorial Board | About | Subscribe | Advertise | Contact | Site Map

PNAS
Proceedings of the National Academy of Sciences of the United States of America

Current Issue | Archives | Online Submission

GO advanced search >>

Institution: FRITZ COMPANIES C/O TELDAN Sign In as Member / Individual

Nathan *et al.* 10.1073/pnas.0503048102.

This Article

- Abstract

Services

- Alert me to new issues of the journal
- Request Copyright Permission

Supporting Information

Files in this Data Supplement:

Supporting Figure 4

Fig. 4. Seasonal histograms of the measured friction velocity (u_*) during seed dispersal periods fitted to a Weibull distribution.

Supporting Figure 5

Fig. 5. Testing the Eulerian component of CELC against published canopy turbulence data [Finnigan, J. (2000) *Annu. Rev. Fluid Mech.* 32, 519-571] for a wide range of canopy morphologies ranging from sparse (LAI = 2 m^2 m^{-2}) to dense (LAI = 6 m^2 m^{-2}), short (h = 0.75 m) to tall (h = 30 m), and constant to heterogeneous leaf area density profile variation (left column). The canopies tested here include rice, corn, aspen, loblolly pine, Scots pine, and a southeastern Hardwood forest (which is analogous to our study site).

Supporting Figure 6

Fig. 6. Sensitivity analysis for the modeled dispersal distances traveled by uplifted seeds $D_{uplifted}$

normalized by canopy height *h*, with respect to the dimensionless variable $\frac{H_r}{V_t}\frac{u_*}{h}$ for LAI = 1, 2, . . . ,5, where u_* is the friction velocity above the canopy, V_t is the seed terminal velocity, and H_r is the mean seed release height. The solid line is the log-log regression to the model data.

Table 1. Shape and scale parameters of the Weibull distribution fitted to the friction velocity (u_*) calculated from wind velocity measurements recorded at 10-Hz at the tower, 40 m above the floor of a 33-m high forest

Period	Shape parameter *b*	Scale Parameter *c*	R^2	*P* (slope = 0)
Nov 2 – Dec 7, 2000	0.34	1.33	0.94	$< 10^{-5}$
Oct 19 – Dec 28, 2001	0.32	1.37	0.96	$< 10^{-5}$
Nov 6 – Dec 30, 2002	0.40	1.48	0.96	$< 10^{-5}$
Mar 29 – May 17, 2002	0.45	1.47	0.94	$< 10^{-5}$
Nov 2, 2000 – Dec 30, 2002	0.36	1.37	0.96	$< 10^{-5}$

Goodness of fit is evaluated by linear regression (measured = intercept + slope * modeled).

Table 2. Published canopy sublayer velocity measurements collected from a wide range of leaf area density, leaf area index (LAI), and canopy height (*h*)

Canopy type	*h*, m	LAI, m m^{-2}	C_d
Rice	0.72	3.1	0.2
Corn	2.21	2.9	0.3
Aspen	10.0	4.0	0.2*
Loblolly pine	14.0	3.8	0.2

Scots pine	20.0	2.0	0.2
Oak-hickory-pine	23.0	5.0	0.15

The published drag coefficient C_d is also shown. All model calculations are conducted assuming standard atmospheric surface layer values for A_u (= 2.7), A_u (= 2.4), A_w (= 1.25) (e.g., ref. 1), and for a = 0.06 (1).

*The value is assumed.

1. Finnigan, J. (2000) *Annu. Rev. Fluid Mech.* **32,** 519-571.

This Article

- **Abstract**

Services

- **Alert me to new issues of the journal**
- **Request Copyright Permission**

Current Issue | Archives | Online Submission | Info for Authors | Editorial Board | About
Subscribe | Advertise | Contact | Site Map

Copyright © 2005 by the National Academy of Sciences

Supporting Methods

The Mathematical Description of the Coupled Eulerian-Lagrangian Closure (CELC) Model

The primary objective of CELC is to generate instantaneous turbulent velocity excursions to simulate the three-dimensional trajectory of wind-dispersed seeds and to estimate the resulting dispersal kernels for a mean velocity (or shear stress) measured or specified above the canopy. The averaging interval in CELC must be sufficiently long to capture an ensemble of eddy turnovers in time, but sufficiently short so that transients in the mean wind do not contribute to velocity excursions (i.e., all departures from time averages are attributed to turbulence). Often, ½ hour averaging periods are deemed optimum. For dispersal simulations longer than ½ hour, ½ hour measured u_* above the canopy are used to drive the model.

Notation Convention. Throughout, our notation convention is as follows. Subscripts denote components of Cartesian tensors and both meteorological and index notations are also used interchangeably (i.e., the components of $\vec{x}$ are $x_1 \equiv x$, $x_2 \equiv y$, and $x_3 \equiv z$) with x, y, and z representing the longitudinal, lateral, and vertical axes, respectively; u_i denote the components of the instantaneous velocity vector $\vec{u}$, with $u_1 \equiv u$, $u_2 \equiv v$, and $u_3 \equiv w$. Generally, index notation is commonly used in theoretical developments, but meteorological notation is often used when reporting field-measurements or idealized flow conditions.

We follow conventional meteorological notation to distinguish among different methods of averaging. Angular brackets (e.g., $< u >$) indicate averaging over space, while over-bar (e.g., $\overline{u}$) indicates averaging over time (e.g., over a 30 min period). Turbulent fluctuations from the time-averaged quantities are denoted by primes (e.g., u'). Based on this convention, recall that the axes are rotated every 30 min so that the longitudinal direction (x_1) is aligned along the mean wind direction and that $\overline{\mathrm{v}}$ = 0.

The trajectory of a seed having a known terminal velocity V_t and released at time t_o from position $x_i(t_o)$ is given by:

$$x_i(t + dt) = x_i(t) + \int_t^{t+dt} (u_i - V_t \delta_{i3}) dt \, , \; i = 1,2,3$$

where u_i are the instantaneous velocity components, dt is the time interval, and δ_{ij} is the Kronecker delta given by:

$$\delta_{ij} = \begin{cases} 1 & for\ i = j \\ 0 & otherwise \end{cases}$$

(i.e., V_t only applies to the vertical component).

The Lagrangian Component. After Thomson's (1) seminal work, Lagrangian stochastic models for the trajectories of particles in turbulent flows are now routinely used in computational fluid mechanics and turbulence research (2). These models are derived using the so-called well mixed condition (*wmc*), which states that if a concentration of a scalar material is initially uniform at some time t_o it will remain so at any future time t in the absence of sources and sinks. The well mixed condition is considered the most rigorous theoretical framework for computing Lagrangian trajectories and ensures consistency with prescribed Eulerian velocity statistics. Using the *wmc*, Thomson (1) showed that in a vertically inhomogeneous turbulence, a set of three stochastic differential equations for the velocity components, given by:

$$du_1' = \left[-\frac{C_o < \varepsilon >}{2}\left(\lambda_{11}u_1' + \lambda_{13}u_3'\right) + \frac{\partial < \overline{u}_1 >}{\partial x_3}u_3' + \frac{1}{2}\frac{\partial < \overline{u_1'u_3'} >}{\partial x_3}\right]dt + \left[\frac{\partial < \overline{u_1'u_1'} >}{\partial x_3}\left(\lambda_{11}u_1' + \lambda_{13}u_3'\right) + \frac{\partial < \overline{u_1'u_3'} >}{\partial x_3}u_1' + \lambda_{33}u_3'\right]\frac{u_3'}{2}dt + \sqrt{C_o < \varepsilon >}\ d\Omega$$

$$du_2' = \left[-\left(\frac{C_o < \varepsilon >}{2} + \frac{1}{2}\frac{\partial < \overline{u_2'u_2'} >}{\partial x_3}u_3'\right)\left(\lambda_{22}u_2'\right)\right]dt + \sqrt{C_o < \varepsilon >}\ d\Omega$$

$$du_3' = \left[-\frac{C_o < \varepsilon >}{2}\left(\lambda_{13}u_1' + \lambda_{33}u_3'\right) + \frac{1}{2}\frac{\partial < \overline{u_3'u_3'} >}{\partial x_3}\right]dt + \left[\frac{\partial < \overline{u_1'u_3'} >}{\partial x_3}\left(\lambda_{11}u_1' + \lambda_{13}u_3'\right) + \frac{\partial < \overline{u_3'u_3'} >}{\partial x_3}\left(\lambda_{13}u_1' + \lambda_{33}u_3'\right)\right]\frac{u_3'}{2}dt + \sqrt{C_o < \varepsilon >}\ d\Omega$$

can be used to model the turbulent excursions, where u_i' are the (instantaneous) turbulent velocities at position x_i and time t, C_0 ($\approx$ 5.5) is a similarity constant (related to the Kolmogorov constant) and λ_{11}, λ_{13}, λ_{22}, and λ_{33} can be derived by inverting the Reynolds stress tensor, and are given by:

$$\lambda_{11} = \frac{1}{< \overline{u_1'u_1'} > - \dfrac{< \overline{u_1'u_3'} >^2}{< \overline{u_3'u_3'} >}}$$

$$\lambda_{22} = < \overline{u_2'u_2'} >^{-1}$$

$$\lambda_{33} = \frac{1}{< \overline{u_3'u_3'} > - \dfrac{< \overline{u_1'u_3'} >^2}{< \overline{u_1'u_1'} >}}$$

$$\lambda_{13} = \frac{1}{< \overline{u_1'u_3'} > - \dfrac{< \overline{u_1'u_1'} >< \overline{u_3'u_3'} >}{< \overline{u_1'u_3'} >}}$$

Here, $< \overline{u_1} >$ is the mean longitudinal velocity (defined so that $< \overline{u_2} >= 0$), $<\overline{u_1'u_1'}>$(= σ_u^2), $<\overline{u_2'u_2'}>$(= σ_v^2) and $<\overline{u_3'u_3'}>$(= σ_w^2) are the variances of the three velocity components, $<\overline{u_1'u_3'}>$ ($= <\overline{w'u'}>$) is the Reynolds stress, and $<\bar{\varepsilon}>$ is the mean turbulent kinetic energy dissipation rate (3, 4). To compute λ_{ij}, it is necessary to model (or measure) the vertical distribution of the flow statistics $<\overline{u_1}>$, $<\overline{u_1'u_1'}>$, $<\overline{u_2'u_2'}>$, $<\overline{u_3'u_3'}>$, $<\overline{u_1'u_3'}>$, and $<\bar{\varepsilon}>$ (Fig. 1). These statistics can be readily computed from Eulerian second-order closure models (5-9). With these velocity statistics, and for the purposes of estimating dt, we define the relaxation time scale (T_L) by

$$T_L = \frac{0.5\times\left(\sigma_u{}^2+\sigma_v{}^2+\sigma_w{}^2\right)}{<\bar{\varepsilon}>}$$

and set $dt = 0.01T_L$ in all model calculations. This estimate of dt satisfies all of the theoretical constraints discussed in ref. 1.

The Eulerian Component. To determine $<\overline{u_1}>$, $\sigma_u{}^2$, $\sigma_v{}^2$, $\sigma_w{}^2$, $<\overline{w'u'}>$, and $<\bar{\varepsilon}>$ for the Lagrangian calculations (Fig. 1) using measured leaf area density and u_*, the Massman and Weil (8) Eulerian second-order closure model is used.

The Massman and Weil Analytical Model. Assuming an exponential mean velocity profile for $z/h < 1$, given by

$$\frac{<\bar{u}(z)>}{<\bar{u}(h)>} = e^{-n\gamma(z)}$$

results in

$$\frac{<\overline{w'u'}(z)>}{u_*{}^2} = e^{-2n(\gamma(z))}$$

$$\frac{\sigma_u}{u_*} = A_u\, \upsilon_1 \frac{\sigma_e(z)}{u_*}$$

$$\frac{\sigma_v}{u_*} = A_v\, \upsilon_1 \frac{\sigma_e(z)}{u_*}$$

$$\frac{\sigma_w}{u_*} = A_w\, \upsilon_1 \frac{\sigma_e(z)}{u_*}$$

where:

$$\frac{\sigma_e}{u_*} = \left[\upsilon_3 e^{-\Lambda\varsigma(h)\gamma(z)} + B_1\left(e^{-3n\gamma(z)} - e^{-\Lambda\varsigma(h)\gamma(z)}\right)\right]^{1/3},$$

$$\gamma(z) = 1 - \frac{\varsigma(z)}{\varsigma(h)},$$

$$\varsigma(z) = \int_0^z C_d\, a(z)dz$$

and the constants are given by

$$n = \frac{1}{2}\left(\frac{u_*}{<\bar{u}(h)>}\right)^{-2}\varsigma(h),$$

$$B_1 = \frac{-9\dfrac{u_*}{<\bar{u}(h)>}}{2\alpha\upsilon_1\left[\dfrac{9}{4} - \Lambda^2\dfrac{{u_*}^4}{(<\bar{u}(h)>)^4}\right]},$$

$$\Lambda^2 = \frac{3\upsilon_1}{\alpha^2},$$

$$\upsilon_1 = (A_u{}^2 + A_v{}^2 + A_w{}^2)^{-1/2},\ \upsilon_3 = (A_u{}^2 + A_v{}^2 + A_w{}^2)^{3/2},\text{ and } \upsilon_2 = \frac{\upsilon_3}{6} - \frac{A_w{}^2}{2\upsilon_1}.$$

The Massman and Weil model (MW99) computes the zero displacement height from the centroid of the momentum sink using:

$$\frac{d}{h} = 1 - \int_0^1 \left(\frac{<\overline{u'w'}(r)>}{u_*{}^2} \right) d(r),$$

where $r = z/h$.

Above the canopy, the flow is assumed to attain its atmospheric surface layer state with

$$\frac{\overline{u'w'}}{u_*{}^2} = -1,\ \frac{\bar{u}}{u_*} = \frac{1}{\kappa}\log\left[\frac{z-d}{z_o}\right],\text{ and } \frac{\sigma_u}{u_*} = A_u\ ,\ \frac{\sigma_v}{u_*} = A_v\ ,\ \frac{\sigma_w}{u_*} = A_w,\text{ where}$$

$$\frac{z_o}{h} = \left(1 - \frac{d}{h}\right) e^{-k_v \frac{\bar{u}_h}{u_*}}.$$

For this study, we used the long-term sonic anemometer data above the canopy during the dispersal seasons and determined that $A_u = 2.1$, $A_v = 1.8$, and $A_w = 1.1$. All of the remaining model parameters of the MW99 formulation can then be determined from these three constants. The estimate of z_o guarantees that a discontinuity in $<\bar{u}>$ does not exist; however, it does not guarantee a well defined $d\bar{u}/dz$ at z/h = 1. This is understandable as the leaf area density is also discontinuous at z/h = 1.

With this model formulation, the leaf area density affects ς and hence $<\overline{\mathrm{u}_1}>$, $\sigma_u{}^2$, $\sigma_v{}^2$, $\sigma_w{}^2$, $<\overline{w'u'}>$, and $<\bar{\varepsilon}>$ profiles, which then can be used to update λ_{11}, λ_{13},

λ_{22}, and λ_{33} and the parameters of the Thomson (1) model if u_* above the canopy is known.

Input Parameters for CELC. The needed parameters for CELC are the leaf area density profile, an estimate of the drag coefficient (assumed = 0.25 here), the measured u_* or $<\overline{u_1}>$ above the canopy every ½ hour, the seed terminal velocity and release height. The leaf area density was measured by a Licor LAI 2000 canopy analyzer, the drag coefficient was estimated from Katul *et al.* (10), and the $<\overline{u_1}>$ above the canopy was measured using a triaxial sonic anemometer at 10 Hz and averaged every 30 min. The other biological parameters needed in the Lagrangian component of CELC were estimated as follows.

Trees were mapped on a 2.5-m grid, and measured for DBH (diameter at a height of 1.3 m). Adults were defined as those having DBH ≥15 cm for all species except *C. caroliniana*, for which we set a threshold of 7 cm. For a sample of at least 15 adult trees of each species, we measured tree height, and fitted least square semilogarithmic regression against basal area. Slopes of all regressions were significantly greater than zero ($P < 0.001$ in all cases) and basal area explained 61–85% of variance in tree height. We estimated height from basal area using the fitted function for trees whose heights were not measured. For each species, we estimated the vertical distribution of seed release by counting seeds or inflorescences along tree height for at least five trees. On the basis of these observations, we calculated the mean release height. The mean and variance of seed terminal velocity was measured by analyzing video photos of falling seeds (collected at the study site) in a closed room in the laboratory with still air conditions, for at least 100 seeds per species.

Computations of Seed Dispersal with CELC. The calculation of seed trajectories proceeds as follows:

1. The flow statistics $<\bar{u}>$, $<\overline{u'^2}>$, $<\overline{v'^2}>$, $<\overline{w'^2}>$, $<\overline{u'w'}>$ and $<\bar{\varepsilon}>$ are calculated by the MW99 model using the measured leaf area density, assumed drag coefficient (C_d = 0.25), and the measured friction velocity (u_*) above the canopy every 30 min.
2. The terminal velocity for each dispersal event was randomly selected from a Gaussian distribution, following previous generalizations (11, 12), based on the measured mean and standard deviation for each species. The number of seeds released per tree for each 30-min period was constant, and was assumed to be linearly proportional to the tree basal area (13). The overall number of dispersal events simulated for each season was of the order of 10^6-10^7 seeds per species. The vertical distribution of seed release heights was assumed to follow a Gaussian distribution around the estimated mean release height, and the standard deviation was bounded symmetrically by the distance from the tree top to this centroid.
3. Given a specified seed release coordinates and terminal velocity, the concomitant velocity fluctuations and seed trajectories are calculated from Thomson's model using the flow statistics in step 1 with x_1 aligned along the measured mean wind direction above the canopy for this 30 min interval.

Testing the Stationarity of the Friction Velocity During Dispersal Seasons and Across Years

To test whether the friction velocity (u_*) above the canopy is stationary, we computed its histogram for each dispersal season using ≈2 months of 30-min u_* data (i.e., >750 data points). Each histogram was then fitted to a 2-parameter Weibull probability density function (pdf), given by

$$pdf\,(u_*) = \frac{c\,{u_*}^{c-1}}{b^c}\exp\left(-\left[\frac{u_*}{b}\right]^c\right)$$

where b and c are shape and scale parameters, respectively. Hence, if b and c are approximately the same across dispersal seasons and years, then u_*, the key forcing variable to dispersal, can be treated as stationary. Using maximum likelihood techniques, these two parameters were fitted by solving two nonlinear equations:

$$b = \left[\frac{1}{n} \sum_{i=1}^{n} [u_*(i)]^c \right]$$
$$c = \frac{n}{\left(\frac{1}{b}\right)^c \sum_{i=1}^{n} [u_*(i)]^c \log(u_*(i)) - \sum_{i=1}^{n} \log(u_*(i))}$$

where $u_*(i)$ ($i =$ 1, 2, …n) are the measured u_* time series, and n is the number of u_* measurements per period (2 months). The Weibull distribution was chosen in favor of other alternative functions because of its broad usage in numerous applications including wind atlases (14), wind energy (15), fire spread (16), and climate change (17).

The Weibull function fitted very closely the measured u_* time series (Fig. 4) for each period (Table 1; R^2 values ranging from 0.94 to 0.96; $P_{(\text{slope = 0})} < 10^{-5}$ in all cases). The observed and fitted histograms for the 5 periods (Fig. 4) and the fitted values of the shape and scale parameters (Table 1), clearly show that the seasonal variation in u_* is minor as compared to the 5-fold (1 to 5) seasonal variation in LAI. Thus, as first-order approximation, u_*, the key forcing term in the CELC model, can be considered as stationary with respect to the seasonal variation in foliage density.

Testing the Massman-Weil Eulerian Model for Various Canopy Types

To verify whether the Eulerian component of CELC correctly describe wind flow patterns under the widest possible range of foliage densities, we assembled data from six studies carried out in a variety of ecosystems (Table 2). These data sets cover both sparse and dense canopies (LAI ranged from 2 to 6 m^2 m^{-2}), short and tall canopies (h ranges from 0.75 to 30 m), and simple and complex leaf area density distribution; for example, the leaf area density profile of a rice canopy is known to be nearly constant, while that of a loblolly pine forest is usually erratic (see refs. 5 and 9 for examples).

We also tested the Eulerian model against wind data collected in our study site. For this comparison, we focus on two approximate ends of the expected LAI variation in a typical temperate deciduous forest: late fall season (November) with low foliage density (LAI = 1.6 m^2 m^{-2}) and mid summer season (August) with full foliage (LAI = 4.8 m^2 m^{-2}).

The comparisons between measured and modeled flow statistics for canopies that differ substantially in their structural and morphological attributes (Table 2) demonstrate the model's ability to reproduce the key features of wind flow patterns (Fig. 5; R^2 values ranging from 0.60 to 0.92 for the four flow statistics, $P_{(\text{slope} = 0)} < 10^{-5}$ in all cases). We also found good agreement between the measured and modeled flow statistics for our study site (R^2 values ranging from 0.71 to 0.93, $P_{(\text{slope} = 0)} < 0.01$ in all cases). Altogether, these results show that CELC's Eulerian component is able to relate variation in foliage density, as represented by LAI, to the corresponding variation in the major flow statistics.

Sensitivity Analysis on Mean Dispersal Distance of Uplifted Seeds (D_{uplift})

From the log-log plots in Fig. 6, the mean distance traveled by uplifted seeds ($< D_{uplift} >$, angular bracket is averaging over all dispersal distances for seeds that experienced uplifting) were shown to be well approximated by power laws of $\xi = \dfrac{u_*}{V_t}\dfrac{Hr}{h}$, with a multiplier that depends on LAI.

Mathematically, the dependence in Fig. 6 can be expressed as a family of curves given by

$$\frac{< D_{uplift} >}{h} = C_1 f(LAI) \times \left(\frac{u_*}{V_t} \frac{Hr}{h} \right)^{\beta} = C_2 (LAI) \times \left(\frac{u_*}{V_t} \frac{Hr}{h} \right)^{\beta} \quad \textbf{[4.1]}$$

where β is an exponent, C_1 is a constant, and $f(LAI)$ is a scaling parameter.

Based on linear regression analysis of the data in Fig. 6, we found that the 95% confidence intervals for β lie between 0.93 and 1.09. That is, β is sufficiently close to unity. Hence, in a first order analysis, we assume $\beta = 1$. We also found that $\log[C_2(LAI)] \approx \left(2 - 0.15 \times LAI\right)$ (R^2 = 0.93) for LAI ranging from 1 to 5 thereby simplifying the above equation for $< D_{uplift} >$ to

$$< D_{uplift} >= Exp(2 - 0.15\,LAI) \times \frac{u_* \, Hr}{V_t}. \ \mathbf{[4.2]}$$

Hence, with this approximate formulation for $< D_{uplift} >$, it is possible to execute a formal sensitivity analysis on how the relative changes in each of the key variables impacts $< D_{uplift} >$. Using the chain rule,

$$dD_{uplift} = \frac{\partial D_{uplift}}{\partial LAI} dLAI + \frac{\partial D_{uplift}}{\partial u_*} du_* + \frac{\partial D_{uplift}}{\partial V_t} dV_t + \frac{\partial D_{uplift}}{\partial Hr} dHr. \ \mathbf{[4.3]}$$

Using **4.2** to compute the partial derivatives, we obtain:

$$\frac{dD_{uplift}}{D_{uplift}} = \left(\frac{du_*}{u_*} + \frac{dHr}{Hr}\right) - \left(\frac{dV_t}{V_t} + 0.15\,dLAI\right). \ \mathbf{[4.4]}$$

Note that expression **4.4** is related to changes in LAI directly. The reason why LAI does not appear in the denominator is due to the exponential dependence of $< D_{uplift} >$ on LAI. If the differentials are approximated by differences, then

$$\frac{\Delta < D_{uplift} >}{< D_{uplift} >} \approx \left(\frac{\Delta u_*}{u_*} + \frac{\Delta Hr}{Hr}\right) - \left(\frac{\Delta V_t}{V_t} + 0.15\,\Delta LAI\right) \ \mathbf{[4.5]}$$

where Δ indicates a difference or an increment.

Expression **4.5** permits us to assess the most important variable affecting D_{uplift} given the natural variability in u_*, H_r, V_t, and LAI, as reflected by the range of the observed parameter values as measured for our study species and site. We emphasize that this exercise does *not* reflect the entire spectrum of dispersal events but focuses only on the small number of uplifting events. This analysis should therefore be viewed as addressing the following question: *given that a seed has been uplifted*, what is the relative importance of different operative factors in determining the distance it travels?

Based on model simulations, uplifted seeds cover almost the entire measured V_t spectrum, as has been empirically observed (18, 19); hence, we can assume that $\Delta V_t \approx$ 0.8 m s^{-1} (0.7 to 1.5 m s^{-1}), with an average of 1.0 m s^{-1}. Seeds are uplifted mostly from the upper third of the forest canopy, $\Delta H_r \approx 1/3$ (2/3 *h* to h). Summary of u_* values of uplifted seeds in the simulations gives $\Delta u_* \approx 1.4$ m s^{-1} (0.5 to 1.9 m s^{-1}), with an average of 0.8 m s^{-1}. Finally, given the seasonal variability in LAI (Fig. 1), ΔLAI ≈ 4 m^2 m^{-2}. Hence, when we combine these order of magnitude estimates, the effects of u_*, H_r, V_t, and LAI on D_{uplift} are approximately

$$\frac{\Delta\langle D_{uplift}\rangle}{\langle D_{uplift}\rangle} \approx \left(\frac{1.4}{0.8}+\frac{1/3}{0.8}\right)-\left(\frac{0.8}{1.0}+0.15\times 4\right)=1.8+0.4-0.8-0.6=0.8 \quad \textbf{[4.6]}$$

1. Thomson, D. J. (1987) *J. Fluid Mech.* **180,** 529-556.

2. Pope, S. B. (2000) *Turbulent Flows* (Cambridge Univ. Press, Cambridge, U.K.).

3. Raupach, M. R. & Shaw, R. H. (1982) *Boundary-Layer Meteorol.* **22,** 79-90.

4. Finnigan, J. (2000) *Annu. Rev. Fluid Mech.* **32,** 519-571.

5. Katul, G. G. & Albertson, J. D. (1998) *Boundary-Layer Meteorol.* **89,** 47-74.

6. Ayotte, K. W., Finnigan, J. J. & Raupach, M. R. (1999) *Boundary-Layer Meteorol.* **90,** 189-216.

7. Katul, G. G. & Chang, W. H. (1999) *J. Appl. Meteorol.* **38,** 1631-1643.

8. Massman, W. J. & Weil, J. C. (1999) *Boundary-Layer Meteorol.* **91,** 81-107.

9. Katul, G., Lai, C. T., Schafer, K., Vidakovic, B., Albertson, J., Ellsworth, D. & Oren, R. (2001) *Adv. Water Res.* **24,** 1119-1132.

10. Katul, G. G., Mahrt, L., Poggi, D. & Sanz, C. (2004) *Boundary-Layer Meteorol.* **113,** 81-109.

11. Greene, D. F. & Johnson, E. A. (1992) *Am. Nat.* **139,** 825-838.

12. Nathan, R., Safriel, U. N. & Noy-Meir, I. (2001) *Ecology* **82,** 374-388.

13. Clark, J. S., Macklin, E. & Wood, L. (1998) *Ecol. Monogr.* **68,** 213-235.

14. Troen, I. & Petersen, E. L. (1989) *European Wind Atlas* (Riso National Laboratory, Roskilde, Denmark).

15. Jamil, M., Parsa, S. & Majidi, M. (1995) *Renewable Energy* **6,** 623-628.

16. Floyd, M. L., Romme, W. H. & Hanna, D. D. (2000) *Ecol. Appl.* **10,** 1666-1680.

17. Pavia, E. G. & O'Brien, J. J. (1986) *J. Clim. Appl. Meteorol.* **25,** 1324-1332.

18. Horn, H. S., Nathan, R. & Kaplan, S. R. (2001) *Ecol. Res.* **16,** 877-885.

19. Nathan, R., Katul, G. G., Horn, H. S., Thomas, S. M., Oren, R., Avissar, R., Pacala, S. W. & Levin, S. A. (2002) *Nature* **418,** 409-413.

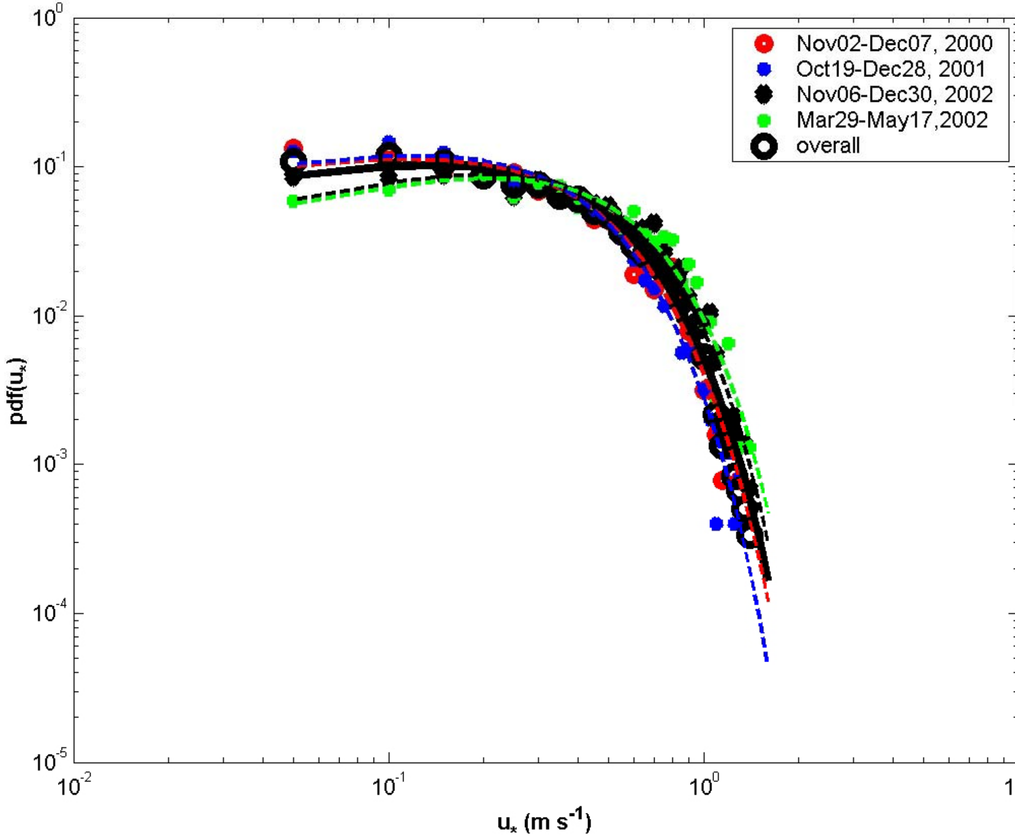

Nov02-Dec07, 2000
Oct19-Dec28, 2001
Nov06-Dec30, 2002
Mar29-May17,2002
overall
pdf(u*)
u* (m s-1)
10^0
10^-1
10^-2
10^-3
10^-4
10^-5
10^-2
10^-1
10^0
10^1

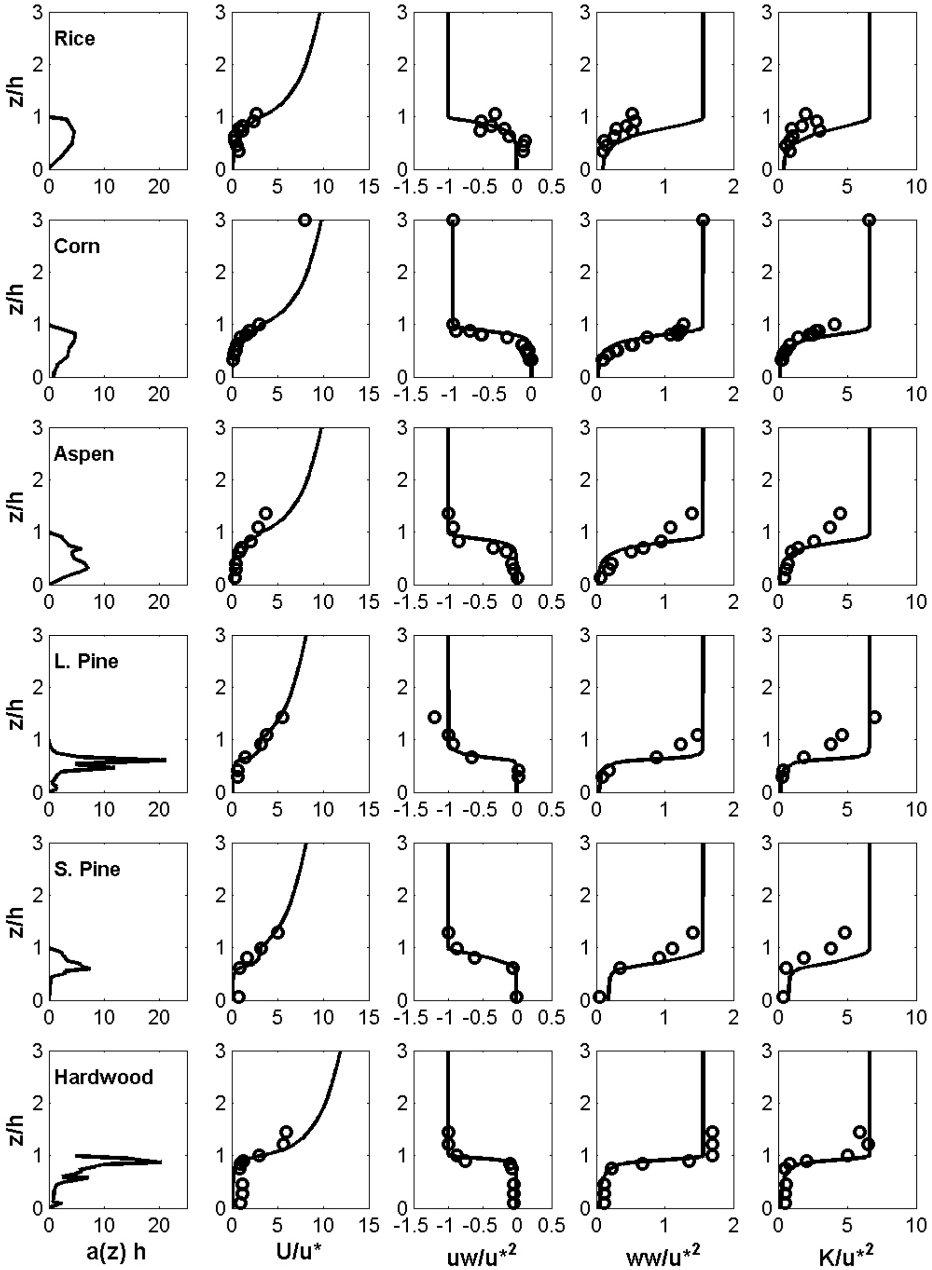
Rice
Corn
Aspen
L. Pine
S. Pine
Hardwood
z/h
a(z) h
U/u*
uw/u*2
ww/u*2
K/u*2

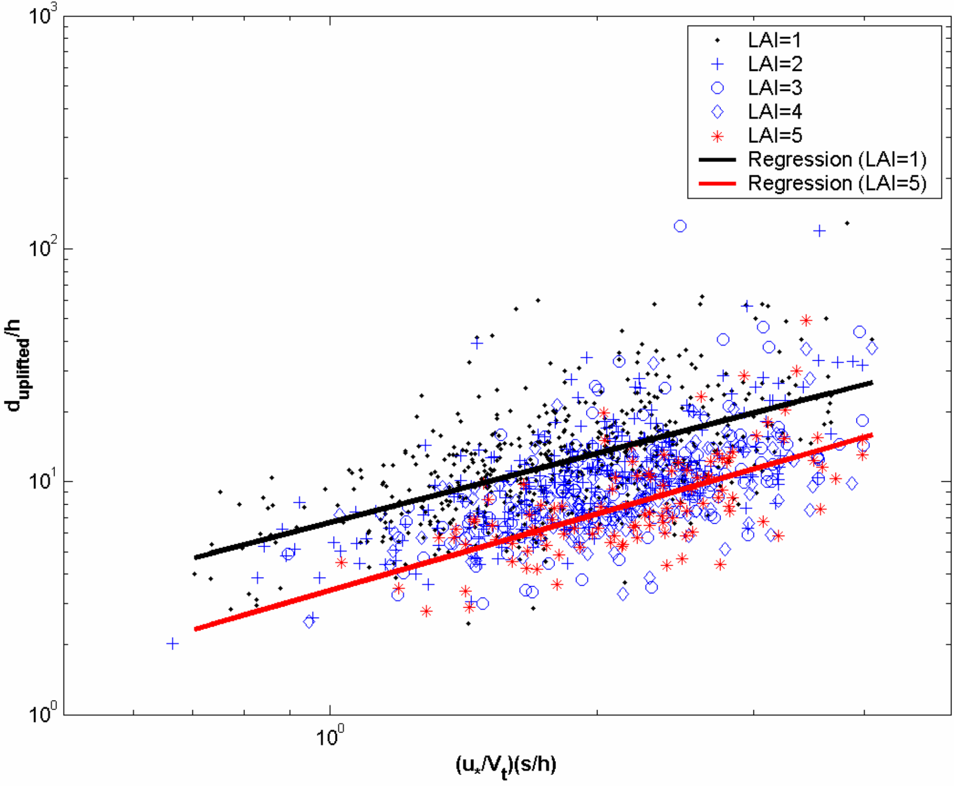

LAI=1
LAI=2
LAI=3
LAI=4
LAI=5
Regression (LAI=1)
Regression (LAI=5)
$d_{uplifted}/h$
$(u_*/V_t)(s/h)$
10^3
10^2
10^1
10^0
10^0